energies

MDPI

Article

Geomechanical and Petrophysical Assessment of the Lower Turonian Tight Carbonates, Southeastern Constantine Basin, Algeria: Implications for Unconventional Reservoir Development and Fracture Reactivation Potential

Rafik Baouche [1], Souvik Sen [2,†] and Ahmed E. Radwan [3,*]

[1] Department of Geophysic, Laboratory of Resources Minérals at Energétiques, Faculty of Hydrocarbons and Chemistry (FHC), University M'Hamed Bougara Boumerdes, Boumerdès 35000, Algeria
[2] Geologix Limited, Dynasty Building, Andheri Kurla Road, Andheri (E), Mumbai 400059, Maharashtra, India
[3] Faculty of Geography and Geology, Institute of Geological Sciences, Jagiellonian University, Gronostajowa 3a, 30-387 Kraków, Poland
* Correspondence: radwanae@yahoo.com or ahmed.radwan@uj.edu.pl
† Current address: Halliburton Consulting, Mumbai 400063, Maharashtra, India.

Abstract: In this study, we assessed the unconventional reservoir characteristics of the Lower Turonian carbonates from the southeastern Constantine Basin. We integrated petrography, petrophysical, and rock-mechanical assessments to infer formation properties and unconventional reservoir development strategies. The studied fossiliferous argillaceous limestones are rich in planktonic foraminifera, deposited in a calm and low energy depositional condition, i.e., deep marine basinal environment. Routine core analysis exhibits very poor porosity (mostly < 5%) and permeability (<0.1 mD), implying the dominance of nano and microporosity. Micritization and calcite cementation are inferred as the major reservoir quality-destroying diagenetic factors. Based on the wireline log-based elastic properties, the upper part of the studied interval exhibits higher brittleness (BI > 0.48) and fracability (FI > 0.5) indices compared to the lower interval. Borehole breakouts indicate ~N-S SHmax orientation and a normal to strike-slip transitional stress state has been constrained based on a geomechanical assessment. We analyzed safe wellbore trajectory and minimum mud weight requirements to ensure stability in the deviated and horizontal wells required for field development. At the present stress state, none of the fracture orientations are critically stressed. We inferred the fracture reactivation potential during hydraulic stimulation required to bring the tight Turonian limestones into production. Additional pore pressure build-up required to reactivate optimally oriented natural fractures has also been inferred to ensure success of hydraulic fracturing.

Keywords: geomechanical characterization; in situ stress; Lower Turonian; unconventional reservoir; tight carbonates; fracture reactivation; Constantine Basin

Citation: Baouche, R.; Sen, S.; Radwan, A.E. Geomechanical and Petrophysical Assessment of the Lower Turonian Tight Carbonates, Southeastern Constantine Basin, Algeria: Implications for Unconventional Reservoir Development and Fracture Reactivation Potential. *Energies* **2022**, *15*, 7901. https://doi.org/10.3390/en15217901

Academic Editor: Mofazzal Hossain

Received: 19 September 2022
Accepted: 12 October 2022
Published: 25 October 2022

1. Introduction

Understanding in-situ stress is critical for efficient and productive development of tight carbonate reservoirs and other unconventional resources. Hydraulic fracturing is an important method for increasing the permeability of rocks and maximizing hydrocarbon recovery in unconventional resources. A better understanding of rock properties, in-situ stress, treatment fluids, and completion strategy can lead to more effective exploitation of unconventional resources. The northern Africa experienced a major eustatic sea-level rise during the Turonian-Cenomanian, which led to an anoxic deep marine condition [1–5]. During this period, organic-rich carbonate sediments were deposited [6]. Farouk et al. [5] reported such a carbonate interval from the Abu Gharadig field, Egypt, where authors studied the self-sourced unconventional reservoir potential of the Lower Turonian Abu Roash-F limestones. Lower Turonian carbonates of the southeastern Constantine Basin of

northern Algeria is another excellent example. There are a very few works that focused on these carbonates from Algeria, especially Constantine Basin. Dokka et al. [7] briefly discussed about the Cenomanian carbonate pay zones from the Guerguett-El-Kihal area of southeastern Constantine. Boudjema et al. [8] reported 1.5–7% total organic carbon content (TOC) and type-II amorphous kerogens within the Cenomanian-Turonian intervals, which are in an oil window. Baouche et al. [9] discussed the petrophysics-based reservoir quality ranking and rock-mechanical properties of the entire Cretaceous interval from the southeastern Constantine Basin. In a recent work, Boutaleb et al. [4] studied the Lower Turonian carbonates of the Djebel Darmoun field located in the southeastern Constantine Basin. These carbonates were deposited during the oceanic anoxic event (OEA2) and authors reported ~1.06 wt% TOC composed of Type-II-III kerogens [4]. However, a detailed study focused on the unconventional reservoir development aspects of the Lower Turonian carbonates was lacking in the literature, which sets the premise of this work.

In this work, we have integrated the available petrographic thin sections, petrophysical measurements from routine core analysis, wireline logs (along with advanced logs like acoustic imaging), and subsurface pressure measurements. We briefly characterized the unconventional reservoir characteristics of the studied Lower Turonian limestones. Under geomechanical analysis, we presented the log-based rock strength, dynamic elastic properties, brittleness index, fracability index, pore pressure, and in-situ stress magnitudes. Based on these rock-mechanical assessment and regional geological understanding, we discussed the unconventional reservoir development aspects which involve horizontal well placement, optimum mud weight requirement to achieve wellbore stability, and fracture reactivation potential due to fluid injection-induced shear slippage. This work is timely and important, given the fact that Algerian operators are looking beyond the long-producing proven conventional reservoirs to increase the resource base, and the outcomes of this work will help the subsurface community to better plan the Lower Turonian unconventional resource exploitation.

2. Geological Setting

The Constantine Basin is situated in the southeastern part of the Saharan Atlas, northern Algeria, close to the Tunisian border [4,9] (Figure 1). The Saharan Atlas is separated from the Saharan platform by the South Atlas fault, which marks the southern boundary of the studied basin. The basin was affected by Cenozoic compressive events pin three phases [10,11]. The basin records clastic sedimentation during the Albian age. Transgression started at the end of Albian age, followed by pelagic carbonate deposition due to Cenomanian transgressive events. The Turonian succession is characterized by carbonates at the base and marl at the top, while the Coniacian, Santonian, and Campanian sedimentation produced chalky and marly limestones [11]. Askri et al. [10] inferred that the Cretaceous carbonates were deposited in a shallow to deep marine conditions, while the marl and shale interbeds may have deposited in tidal flats or restricted lagoonal conditions. Figure 2 illustrates the total petroleum system and the sedimentary section of the studied field. Dokka et al. [7] inferred that the transgressive and organically rich Early Turonian and Albian intervals are the primary source rocks. Boudjema et al. [8] reported Type-II amorphous kerogens from the Cenomanian-Turonian carbonate shales, which exhibit up to 7% total organic carbon content and maturity corresponding to the oil window. In the southeastern Constantine Basin, reservoirs are of mainly Cretaceous age, with oil and gas shows reported from Jurassic, Paleogene, and Neogene units. The oolitic and bioclastic limestones of Upper Cenomanian, Turonian, and Coniacian host reservoir intervals are characterized by 5–15% porosity and 0.1–10 mD permeability [4]. Traps are mostly structural in nature, formed during the tectonic inversion between the Middle Eocene and Oligocene epochs, which resulted in NE-SW folding.

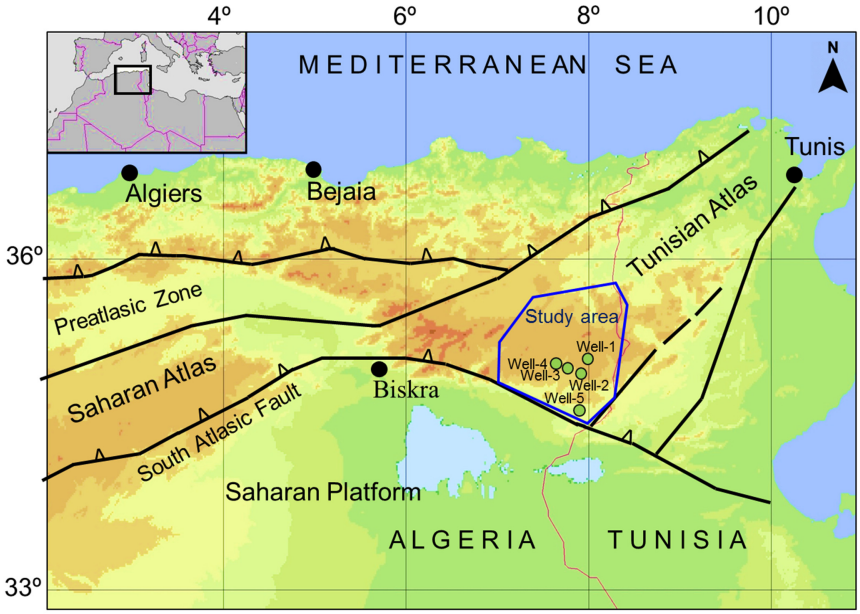

Figure 1. Location map of the southeast Constantine Basin (brown polygon) in northern Algeria. The studied well locations are marked by red circles. Black lines indicate regional structural trends (refer to Baouche et al. [9] for structural trends).

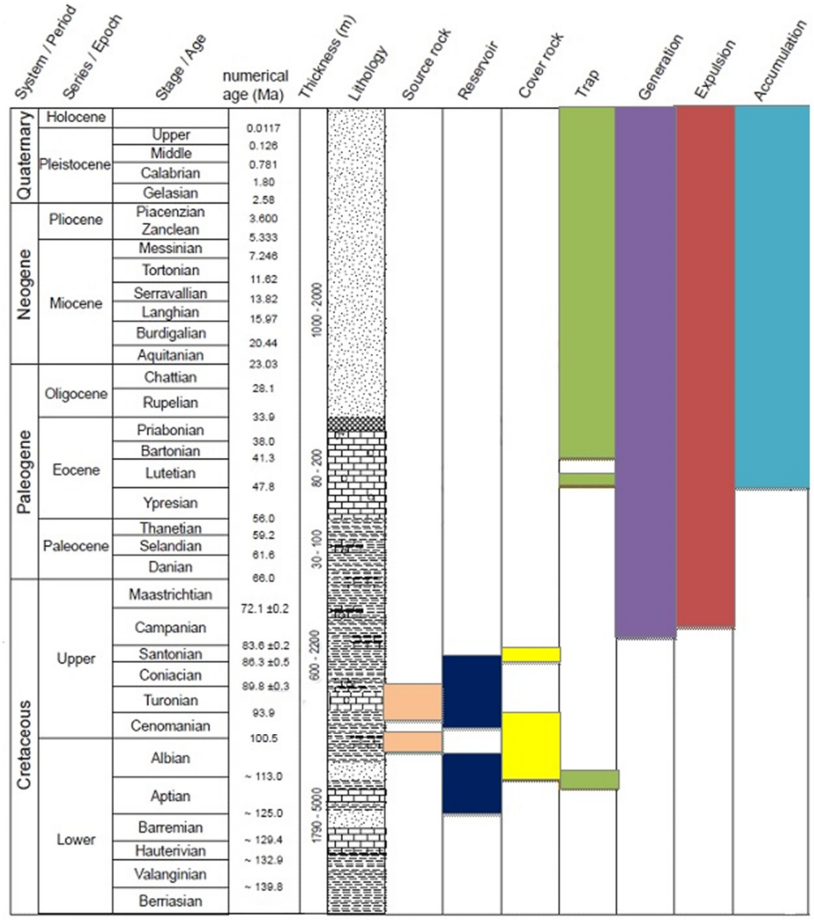

Figure 2. Lithostratigraphic column and the total petroleum system of the southeast Constantine Basin in northern Algeria (for details, please refer to Bentaalla-Kaced et al. [11] and Boutaleb et al. [4]).

3. Materials and Methods

We studied the Turonian carbonate interval from five vertical exploratory wells drilled in the southeastern Constantine Basin.

3.1. Petrographic and Petrophysical Analysis

Cores and thin sections were available from three wells which were evaluated for petrographic characterization. Under an optical microscope, all rock porosity types and depositional textures found in Lower Turonian carbonates were studied and classified using the classification schemes of Choquette and Pray [12] and Dunham [13], as modified by Embry and Klovan [14]. The most important characteristics of the Lower Turonian carbonate, such as rock texture, matrix, and biota, have been observed under a microscope following Flügel [15]. Under light microscopy, representative, blue-dyed thin sections were used to detect porosity.

Physical properties (porosity and permeability) were obtained from Routine core analysis (RCA) of 250 samples (172 samples from Well-1 and 78 samples from Well-2) prepared by the oil company. Specifically, the core samples were first prepared to have a cylindrical shape with a height and diameter of 2.5 cm. Porosity measures the ratio of the sum of all pore space volumes to the total volume in the rock, which is one of the most important reservoir parameters. It characterizes the ability of a rock to store oil; thus, the accurate acquisition of porosity can provide a reliable parameter for reservoir evaluation. Porosity determined by core analysis is the most accurate mean. In this work, the porosity was measured using a porosimeter. Permeability is one of the most significant parameters used to define the ability of a porous material to allow the flow of fluids through their pore spaces. In this work, the permeability of the samples was measured using the steady-state approach [16]. The petrophysical measurements were performed and chosen along most intervals of the reservoir in the two cored wells to represent the whole intervals. The characteristics of pore types and components in the Turonian carbonate interval were observed using a cross plot of porosity and horizontal permeability.

3.2. Geomechanical Analysis

Understanding the strength and geomechanical properties of a reservoir rock is essential for exploiting hydrocarbon resources [17–20]). In this work, wireline logs have been the primary input for geomechanical assessment. We estimated uniaxial compressive strength (UCS) from compressional sonic slowness (DTCO) following Militzer and Stoll [21]:

$$\mathrm{UCS} = \frac{\left(\frac{7682}{\mathrm{DTCO}}\right)^{1.82}}{145} \quad (1)$$

Rock-mechanical properties, i.e., Poisson's ratio (υ), Young's modulus (E), and coefficient of internal friction (μ) were estimated from bulk-density, compressional, and shear sonic slowness [17]. Based on the log-based dynamic elastic properties, we have estimated the brittleness index of the Turonian interval following Grieser and Bray [22]:

$$\mathrm{BI} = \frac{1}{2}\left[\frac{\mathrm{E} - \mathrm{Emin}}{\mathrm{Emax} - \mathrm{Emin}} + \frac{\upsilon - \upsilon\mathrm{min}}{\upsilon\mathrm{max} - \upsilon\mathrm{min}}\right] \quad (2)$$

where υmin and υmax denote minimum and maximum Poisson's ratio, respectively, as estimated within the studied interval. Similarly, Emin and Emax indicate minimum and maximum Young's modulus, respectively. Fracability Index (FI) was estimated following Jin et al. [23]:

$$\mathrm{FI} = \mathrm{w} * \mathrm{BI} + (1 - \mathrm{w}) * \mathrm{EEn} \quad (3)$$

where w is a weight fraction which varies between 0 and 1. We have assumed 0.5 [23]. EEn is the normalized Young's modulus, which is estimated as:

$$\mathrm{EEn} = \left[\frac{\mathrm{Emax} - \mathrm{E}}{\mathrm{Emax} - \mathrm{Emin}}\right] \quad (4)$$

A higher FI value is indicative of a suitable fracture candidate, while lower values indicate poor candidates for hydrofracturing operation. We inferred the formation pore pressure (PP) from direct measurements. Vertical stress (Sv) and minimum horizontal stress (Shmin) are adapted from Baouche et al. [9], who also provided maximum horizontal stress (SHmax) from poroelastic models, but the estimated output was not calibrated. However, in this study, we have employed a stress polygon approach based on our image log-based observations, which constrained the SHmax in a more confident manner. This approach uses the wellbore compressive and tensile failures to infer stress states by constraining SHmax at a given set of PP, Sv, and Shmin based on frictional faulting mechanism [17]. Based on the interpreted geomechanical parameters and horizontal stress azimuth, we inferred the stability and slip potential of randomly oriented fractures. We also interpreted the additional pressure required to induce slip on the weakest fractures [24,25] following Mohr Coulomb failure criteria. We modeled the additional pressure necessities at various friction coefficient values to understand the operational requirements.

4. Results and Discussions

4.1. Petrographical and Petrophysical Characteristics

The cores of the Turonian carbonate interval exhibit a grey to dark grey color, appear tight and devoid of any visible fractures or moldic, vuggy pores (Figure 3a,b), and are inferred as fossiliferous argillaceous limestones. Petrographic investigation indicates the dominance of micrite matrix along with dominant planktic foraminifera with fragmented bivalves (Figure 3c–f). These are inferred as wackestone-packstone and correlate well with the standard microfacies SMF3 following Flügel [15]. Abundance of planktic foraminifera and absence of benthic foraminifera are indicative of calm and low energy depositional conditions in a deep marine basinal environment. Some of the thin sections exhibit sub-parallel thin fractures filled with calcite cements (Figure 3e,f). Micritization is observed as the dominant diagenetic process, which destroyed reservoir quality. Calcite cementation within the fractures also contributed to the cementation-related porosity loss (Figure 3e,f). On the other hand, some vugs have been noticed in some samples, which indicates that local dissolution has occurred in the Lower Turonian carbonate at the diagenesis stages that contribute to relatively forming meso-macro pore sizes (Figure 3f).

Core-measured porosity and permeability data were available for two wells (Figure 4). Well-1 exhibits a porosity (Φ) range of 0.13–6.9% with horizontal permeability (Kh) varying between 0.0001–0.9 mD. Well-2 shows a narrow range of permeability between 0.06–0.16 mD, while porosity varies between 0.02–6.91%. Figure 4 shows the Winland chart that illustrates the relationship between the horizontal permeability and porosity measured in the two cored-wells (well-1 and well-2). This chart can provide important information about the pore throat radius and their distribution in the rock interval. The majority of the data distribution from these two wells indicate that the studied Turonian carbonates are dominantly characterized by nano-microporosity, have poor porosity (mostly < 5%), and very poor permeability (mostly < 0.15 mD), confirming its tight nature (Figure 4). The measured petrophysical data from well-1 shows a wide range of permeability and porosity, with most points representing a nano-micro pore size and a few minor points representing a meso-macro pore size. On the other hand, the measured petrophysical data from well-2 shows a narrow range of permeability and wide range in porosity, with most points representing micro-meso pore size and a few minor points representing macro-pore size. In terms of permeability and pore throat radius, these findings suggest that the Turonian carbonate in well-2 is of higher quality than that in well-1. This enhancement in pore size in

well-2 is most likely due to strong dissolution diagenesis that occurred in the well-2 facies (see Figure 3f).

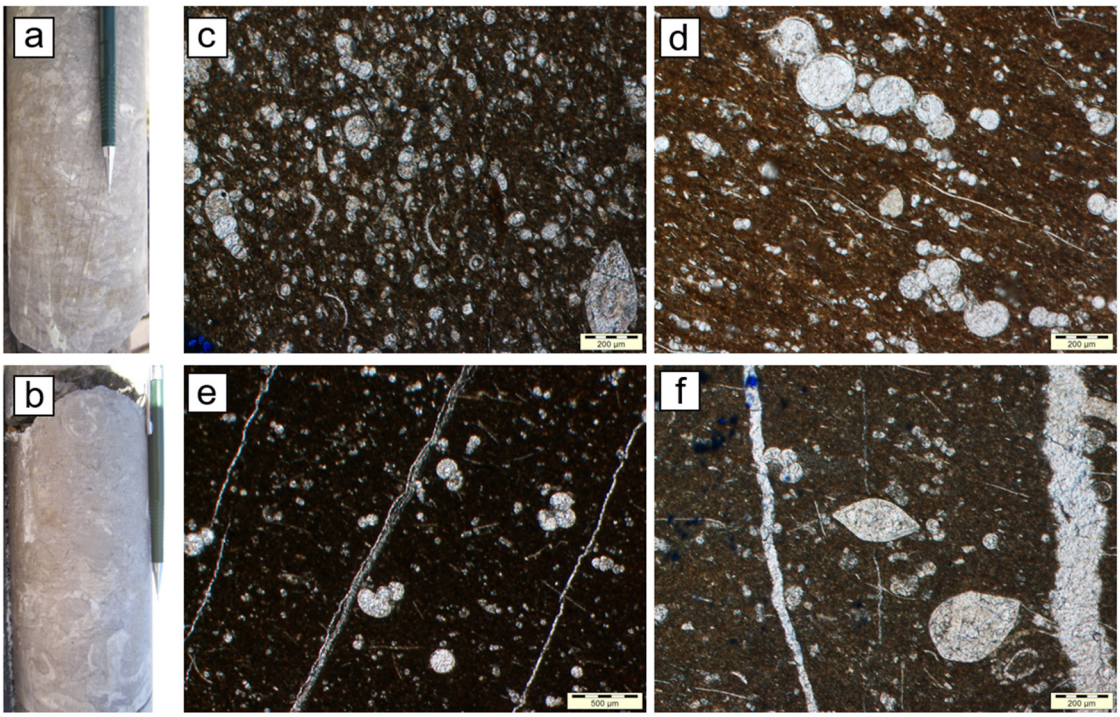

Figure 3. (**a**,**b**) cores of the Turonian carbonate interval taken from Well-1, at depths 1706 m and 1734 m, respectively; thin section petrography indicating (**c**,**d**) planktic foraminiferal wackestone-packstone with fragmented bivalves, dominated by micrite matrix (brown/dark brown colored); (**e**,**f**) planktic foraminiferal wackestone, with scattered planktic foraminiferas, matrix-dominated fractures-filled with calcite cement.

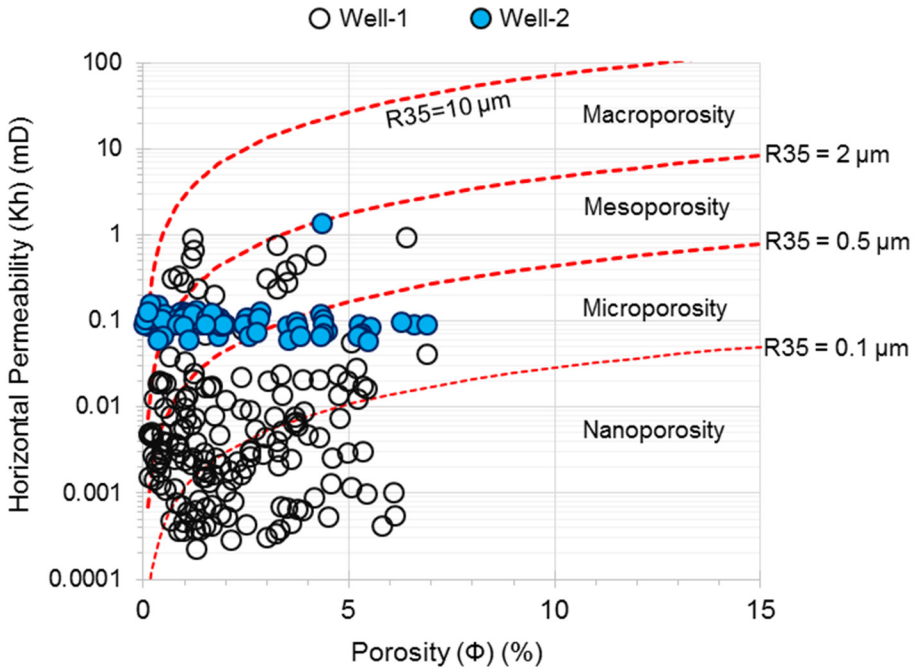

Figure 4. Cross plot between core-measured porosity and horizontal porosity indicating the dominance of nano- and microporosity within the studied Turonian carbonates.

4.2. Rock-Mechanical Properties

Lower Turonian carbonate rock mechanical properties and geomechanical understanding are critical for optimal computational program designs of hydraulic fracturing stimulation, well placement, and completion. Wireline log-based rock strength and elastic properties provided critical insight on Turonian carbonate properties (Figure 5). UCS mostly varies between 35–70 MPa, while the highest UCS was recorded as 95 MPa. Coefficient of internal friction (μ) was observed to vary between 0.65–0.8. Dynamic Poisson's ratio (υ) and Young's modulus (E) exhibit the ranges of 0.29–0.36 and 23–55 GPa, respectively. Based on the log-based dynamic elastic properties, BI was modeled, which provided a wide range of 0.2–0.68 (Figure 5). Brittleness indices show significant variations in the Upper Carbonate Interval and Lower Carbonate Interval, as indicated by elastic properties-based BI. A close observation indicates consistently higher BI (>0.48) at the top part of the Turonian, which represents brittle behaviour, which is associated with higher E and lower υ. In the deeper interval, BI decreased and stayed between 0.2–0.4 dominantly. It mostly shows 'less brittle' behaviour (Figure 5). The BI and E-based Fracability index provided a range of 0.25–0.75. The more brittle top interval is also characterized by high FI values, exceeding 0.5, while the less ductile to less brittle Lower Turonian interval is characterized by FI < 0.5 (Figure 5). Based on the BI and FI estimates, the top part of the Turonian section is a more suitable candidate for hydrofracturing. We correlated the estimated BI values in all the studied wells, presented in Figure 6. All wells exhibited similar brittleness and fracability signatures with depth and indicated high BI–high FI behaviour in the upper Turonian interval, thus providing a suitable candidate correlation. Turonian carbonate's lower interval has higher gamma ray and sonic values than the upper interval. The most likely explanation for this relationship is that the lower interval has more argillaceous content than the upper interval, giving the lower interval a less-ductile to less-brittle nature.

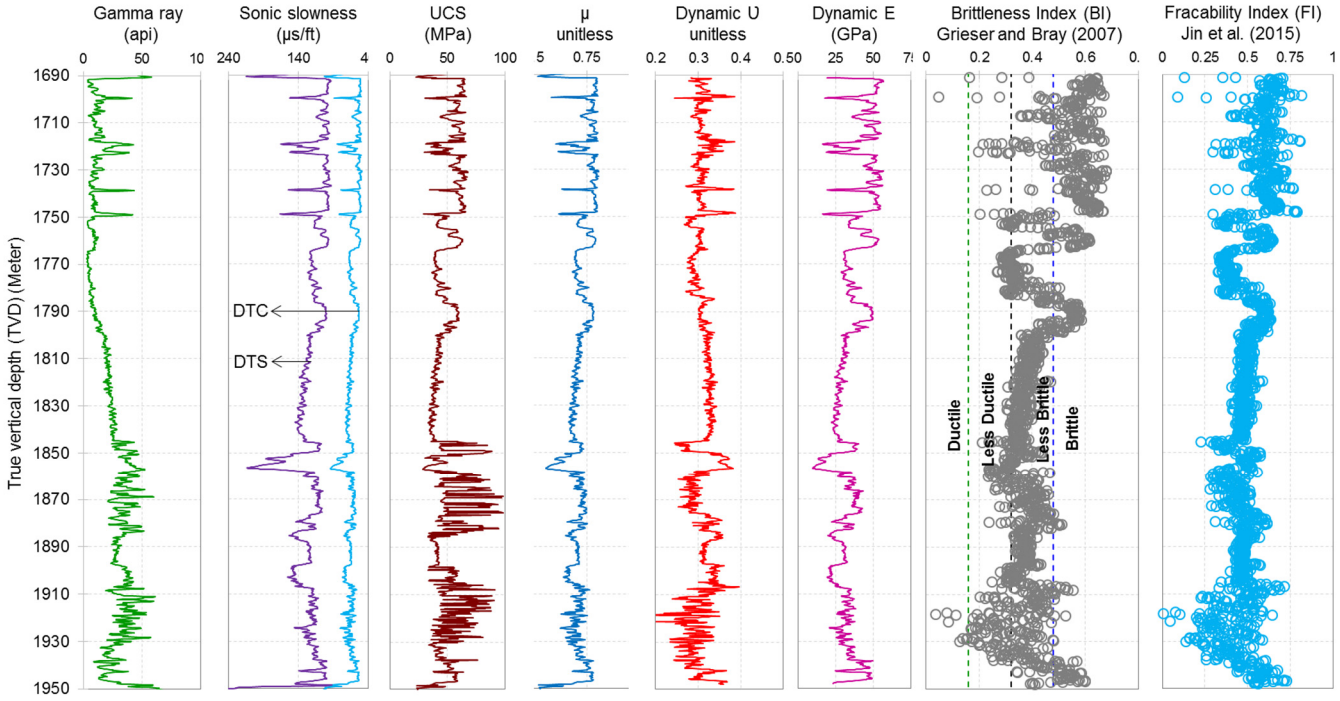

Figure 5. Estimated unconfined compressive strength (UCS), coefficient of internal friction (μ), Poisson's ratio (υ), Young's modulus (E), brittleness index (BI), and Fracability index (FI) of the studied Turonian carbonate interval in Well-1. BI is modeled following Grieser and Bray [22] and FI is estimated as per Jin et al. [23].

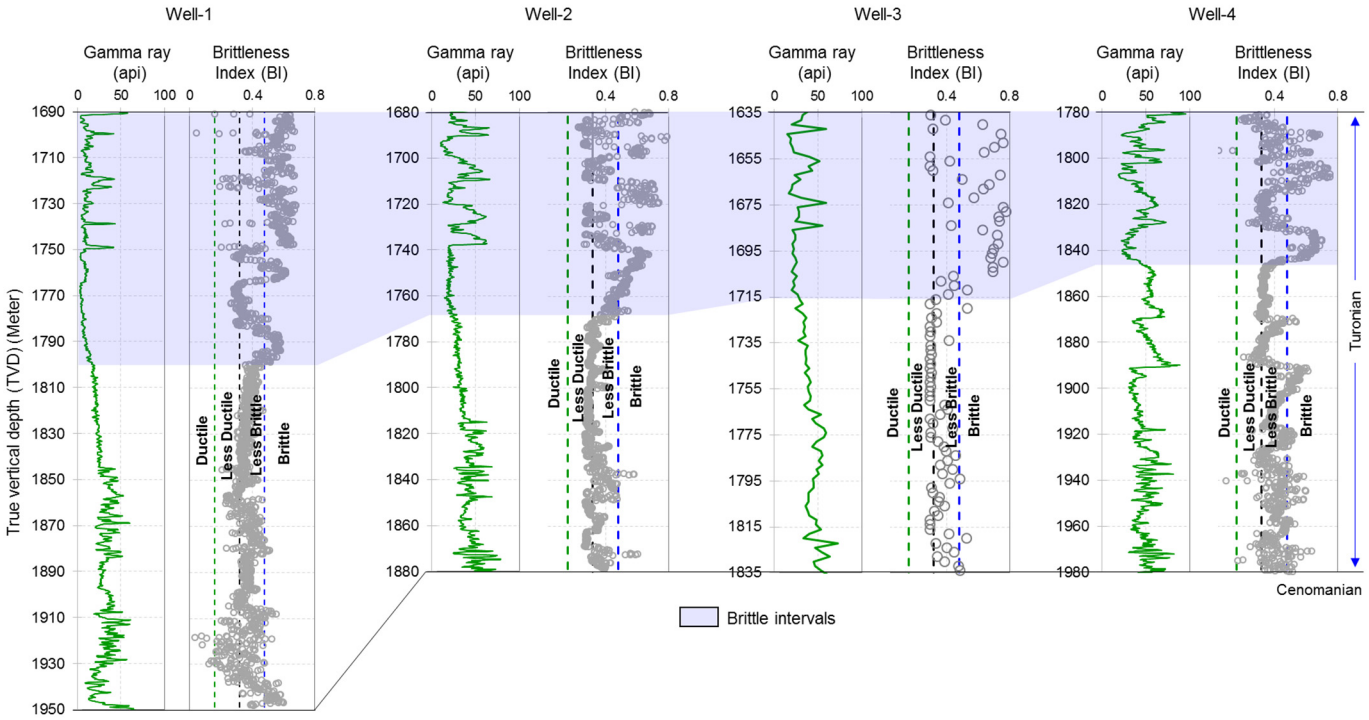

Figure 6. Estimated BI of the studied Turonian carbonates in the four studied wells indicating higher brittleness in the top of the Turonian interval.

4.3. In-Situ Stress State

The determination of in-situ stresses and overpressures is one of the critical elements in petroleum industry [19,20,26–31]. The direct measurements exhibit an average of 0.51 PSI/ft pore pressure gradient within the studied Turonian interval (Figure 7). Baouche et al. [9] interpreted the Sv and Shmin gradients as 1.03 and 0.72–0.86 PSI/ft within the Coniacian-Cenomanian interval. Close observation shows that the Turonian interval has a lower Shmin gradient (~0.72 PSI/ft) than the overlying Coniancian and underlying Cenomanian shales (~0.86 PSI/ft) (Figure 7). The bounding shales with higher Shmin than the Turonian carbonates will provide a good fracture barrier to vertical fracture propagation during hydrofrac operation. It is to be noted that the mentioned Shmin is empirically derived following a poroelastic strain model and could not be validated due to the lack of mini-frac or related measurements within the Turonian section. An Acoustic image log exhibited wellbore breakouts, i.e., compressive failures along E-W (Figure 8). Based on the breakout orientations, SHmax azimuth is observed as 170° N [9]. SHmax magnitude was constrained by the stress polygon approach (Figure 8) [17,26,31]. SHmax could have been modeled from breakout widths, however, lack of calibration in Shmin and UCS would incur uncertainties in that approach. Therefore, we utilized the compressive failure criteria in the stress polygon to constrain SHmax. Figure 8 demonstrates the analysis at 2500 m depth in Well-5, where an acoustic image log was recorded. At this depth, Sv and PP were taken from the regional pressure gradients reported by Baouche et al. [9]. Drilling data indicates that this section was drilled with an average drilling mud pressure of 4800 PSI which maintained ~600 PSI downhole mud overbalance in the Turonian section. Due to the lack of core-measured UCS, we considered the log-estimated UCS range which mostly varies between 35 MPa and 70 MPa (Figure 5). Using this information, the stress polygon provided a possible SHmax range of 6500–9000 PSI at a 2500 m depth (Figure 8). The constrained SHmax magnitude range indicates a normal faulting stress state at weaker rocks with low UCS while a strike-slip state can be observed from compressive failures in stronger rocks (~70 MPa UCS) (Figure 8). This inference provides new insight about the Turonian stress state, which was previously reported as the pure strike-slip based on the poroelastic model

by Baouche et al. [9]. It is to be noted that the occurrences of breakouts in the Turonian interval provided a confident SHmax range.

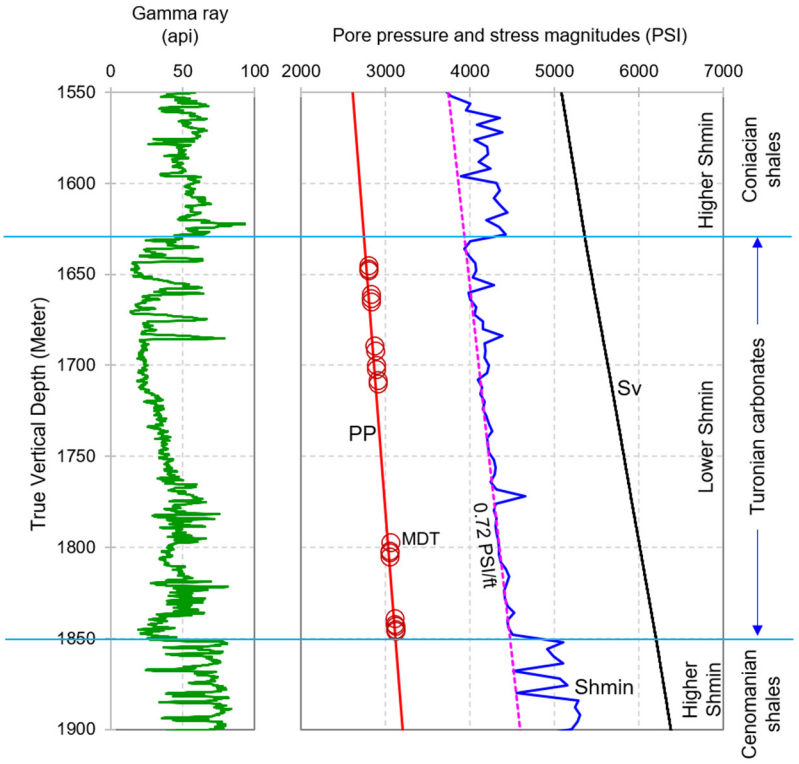

Figure 7. Estimated pore pressure, vertical stress (Sv), and minimum horizontal stress (Shmin) magnitudes in the Turonian carbonates, overburden (Coniancian shales), and under burden (Cenomanian shales), please refer to Baouche et al. [9] for details. Data belongs to Well-1.

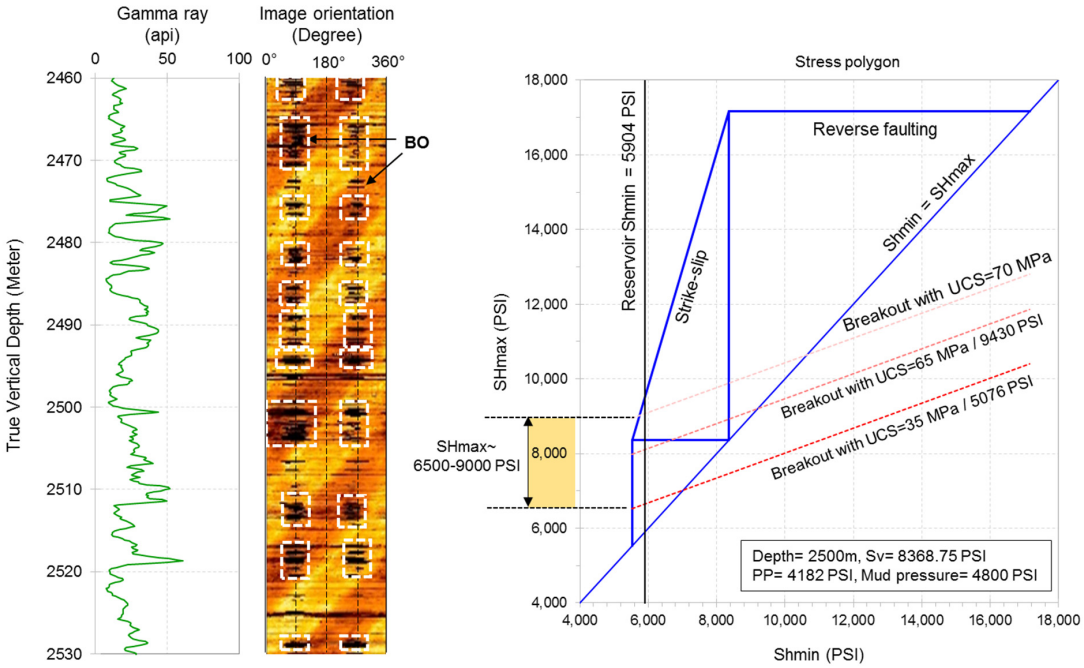

Figure 8. Inferred SHmax azimuth (N170° E) from breakouts (BO) observed in the ultrasonic image log of Well-5 (interpreted BO zones are marked by white boxes); stress polygon approach to constrain SHmax magnitude indicating normal fault to strike-slip tectonic stress state in the Turonian carbonate interval.

4.4. Safe Wellbore Trajectory Analysis

Based on the inferred stresses, we performed the safe wellbore trajectory analysis for optimum azimuths of deviated and horizontal welld within the Turonian carbonates to ensure wellbore stability. With a conservative approach, we considered the allowable breakout as 0°. We have constrained an SHmax range based on the breakout criteria in the stress polygon (Figure 8). The same SHmax magnitude ranges have been considered for trajectory analysis. Results are presented in Figure 9a–d. Considering normal faulting scenarios with SHmax gradients of 0.8 and 0.98 PSI/ft, respectively (Sv > SHmax), horizontal wells along the Shmin azimuth will require 0.61 PSI/ft mud gradient to ensure stability, while laterals drilled parallel to SHmax azimuth will need 0.67 PSI/ft (Figure 9a,b). Deviated wells with inclination less than 30° towards any well azimuth requires the lowest mud weight (<0.54 PSI/ft) to restrict breakouts in normal faulting regime (Figure 9a). In a normal to strike-slip transitional stress state (Sv ~ SHmax > Shmin), any deviated well along SHmax azimuth will require more than 0.67 PSI/ft to achieve stability (Figure 9c), and deviated wells with more than 30° inclination drilled oblique to SHmax can be managed with a 0.60–0.62 PSI/ft mud gradient. In a strike-slip domain, vertical wells are the most unstable ones and require 0.71 PSI/ft mud weight, which is very close to the Shmin gradient (Figure 9d). The wells up to 60° inclination in any direction would require a minimum mud weight of 0.68 PSI/ft mud gradient, while horizontal wells perpendicular to an SHmax direction can be drilled with a 0.63 PSI/ft mud gradient (Figure 9d).

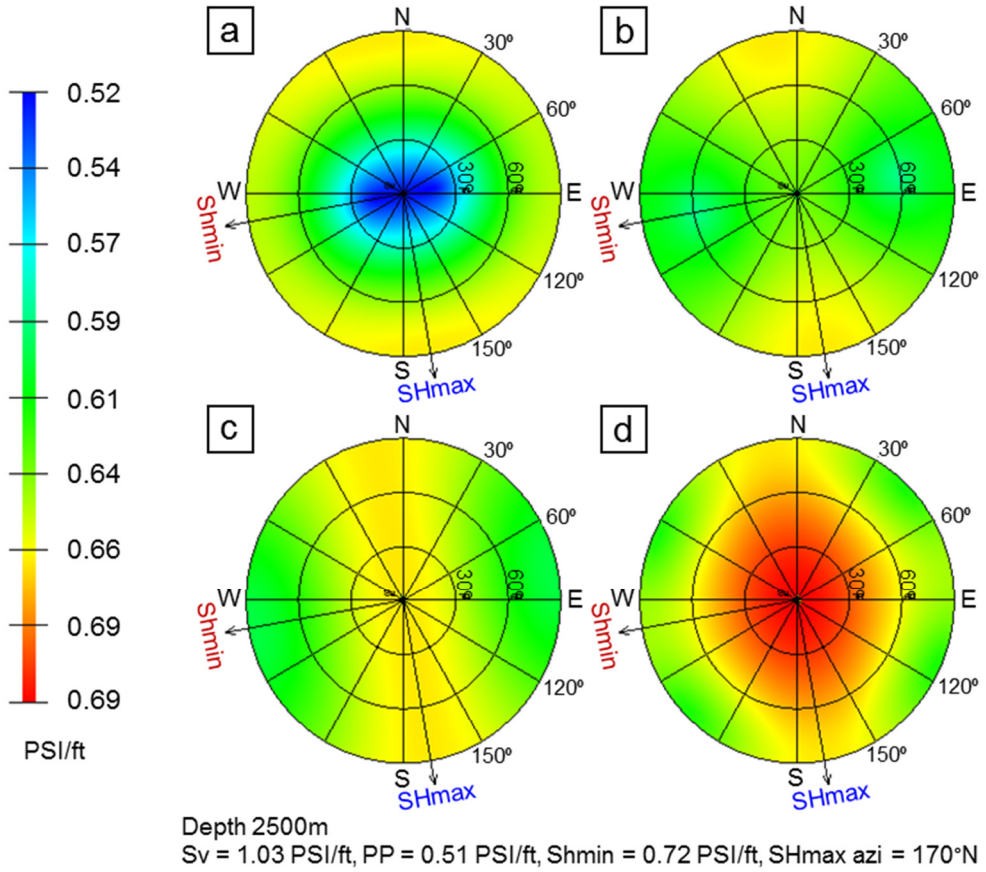

Figure 9. Safe wellbore trajectory analysis and minimum mud weight requirement (Mohr-Coulomb criteria) considering (**a**) SHmax = 0.8 PSI/ft, (**b**) SHmax = 0.98 PSI/ft, (**c**) SHmax = Sv = 1.03 PSI/ft, and (**d**) SHmax = 1.1 PSI/ft (>Sv). In this mud pressure circular plot (lower hemisphere plot), well azimuth is plotted along the periphery of the circle and well inclination is plotted along the radius. Centre of each circle denotes vertical well position.

Considering the range of possible stress states and mud weight requirements in all inclination-azimuth combinations, horizontal wells drilled along the Shmin direction exhibit the lowest mud weight requirement to avoid wellbore compressive failures. A horizontal well parallel to Shmin will also help to create a transverse fracture network by stimulation, which will propagate parallel to SHmax orientation.

4.5. Fracture Reactivation Potential

Due to fluid injection in the hydraulic fracturing process, formation pore pressure increases, and the tendency of existing closed natural fractures to be activated by fluid injection is dependent on their orientations relative to SHmax azimuth [9,19,25,27,28]. The critically stressed fractures are more likely to get reactivated and participate in the flow network. A further increment in pore pressure is capable of reactivating other fracture orientations, thus yielding a reactivated fracture network, which enhances the success of hydraulic fracturing. Since we understood the possibility of tectonic stress state being normal to strike-slip range in the studied Constantine Basin, we analyzed the fracture reactivation potential considering SHmax values of 0.8 PSI/ft (<Sv, normal faulting) and 1.1 PSI/ft (>Sv, strike-slip faulting) with varying coefficients of internal friction (at 0.5, 0.6, and 0.8). The results are presented in Figure 10. The fractures along the Shmin azimuth are the most stable ones and require higher pressure build up to experience shear slippage by fluid injection. Lower μ values reduce the additional pressure requirement for slip. In a normal faulting scenario, a minimum of 950 PSI additional pore pressure will be needed to reactivate optimally oriented natural fractures (Figure 10a–c). The requirement is much less in a strike-slip regime. Considering μ = 0.6, fracture orientations of 10–30° N and 130–150° N can be reactivated with <500 PSI pressure increment (Figure 10d). Clay materials within fractures are capable of reducing μ, and considering μ = 0.5, we observe the orientations of critically stressed fractures as 20–30° N and 130–140° N, while ~500 PSI pressure enhancement by fluid injection can cause slippage on a wide range of fracture orientations (Figure 10f).

4.6. Inferences on Unconventional Reservoir Development

The integration of geology with engineering is necessary to obtain the optimal length and perforation number of unconventional development wells [6]. The relationship should be evaluated between the burial depth, organic-rich lithological thickness, length of the horizontal section, and well production. Petrophysically, the studied Turonian interval exhibits poor storage and very poor flow capacity. We identified frequent thin fractures in the thin sections, which indicate the presence of minor mechanical compaction. These fractures may locally improve the reservoir quality. However, these fractures are seen to be filled with calcite cement, which, therefore, did not improve the flow capacity of the Turonian carbonates. To bring this tight unconventional carbonate reservoir into production, stimulation is certainly required [6]. Horizontal well drilling through the Turonian carbonates with a slotted liner completion strategy is an effective way to ensure maximum reservoir contact, as these perforated liners also provide increased accessibility for CT as well as acid jobs. Hydraulic fracturing is a prime requirement to enhance the flow potential of the tight Turonian. The overall brittle behavior indicates higher hydraulic fracturing success. The upper interval of the Turonian has high BI as well as high FI, which is a more suitable candidate for hydraulic fracturing operation when compared to the lower part of the Turonian.

A complete development plan can be performed through the extraction of geophysical attributes and detailed analysis, and target areas and sweet spots can be determined, highlighting their superior sedimentary and diagenetic conditions, moderate structural uplift and deformation, and good preservation conditions, together with favorable reservoir features such as high brittleness, high porosity and permeability, and high-pressure coefficients. Tailoring the length of horizontal wells and hydraulic fracturing schemes (optimum number of stages, perforations and proppant amount) for the Turonian car-

bonate reservoir and optimizing the hydrocarbon production system are effective ways to maximize the production and its effective development. This study might be the first step toward hydraulic fracturing in the studied region. It should be followed by integrated geological and engineering projects to find suitable methods to improve production and resource recovery.

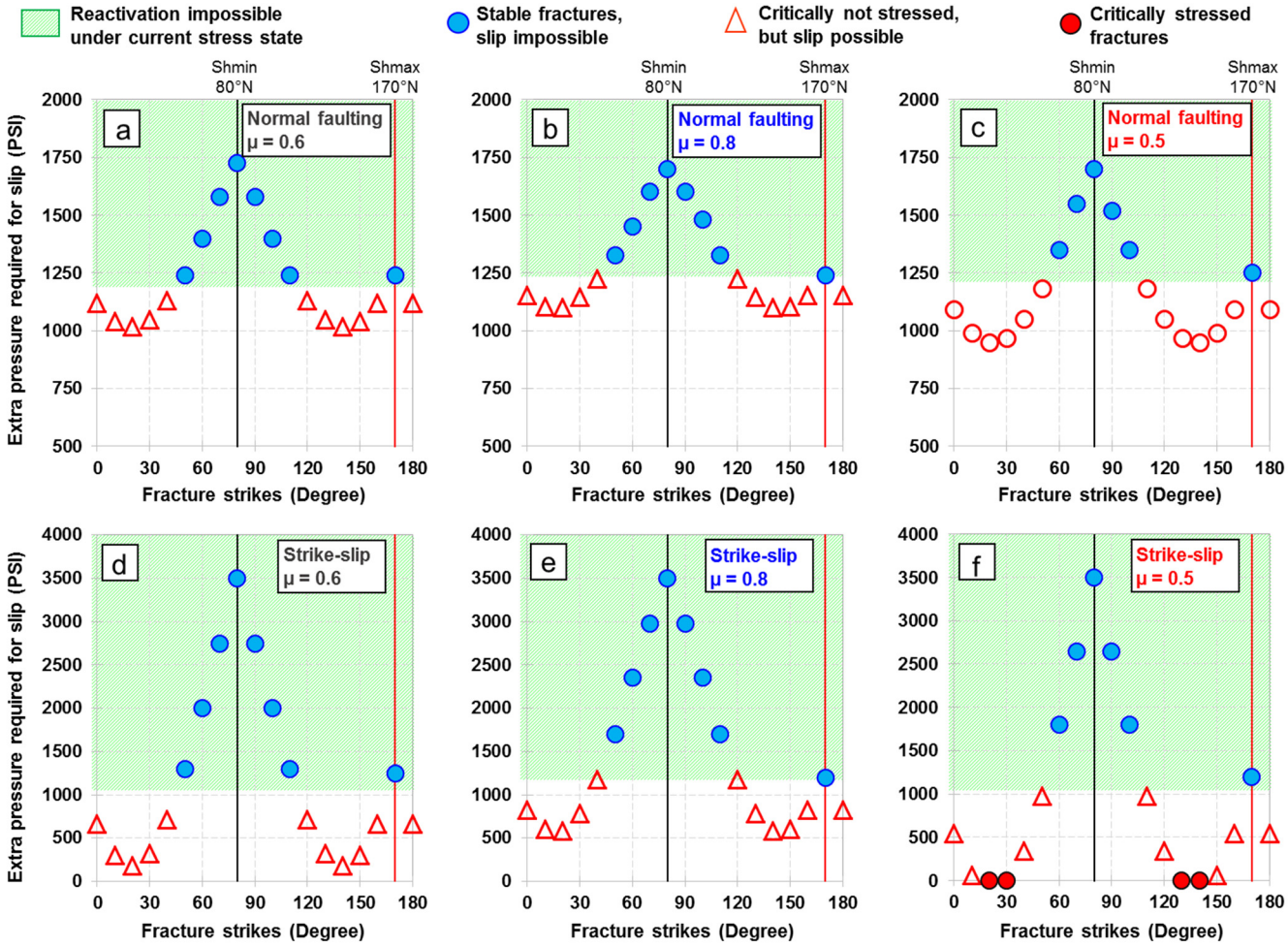

Figure 10. Natural fracture reactivation potential in the Turonian interval considering (**a**–**c**) normal faulting and (**d**–**f**) strike-slip stress regime at various coefficient of internal friction (μ) values.

5. Conclusions

This is the first ever study focused on the unconventional reservoir characteristics of the Lower Turonian carbonates from the southeastern Constantine Basin. Petrographic and petrophysical studies summarize that the studied fossiliferous argillaceous limestones are tight in nature and dominated by nano- and microporosity. The brittleness and fracability of the entire interval have been inferred utilizing the wireline log-based rock-mechanical assessment, which helped to identify the suitable hydrofracturing zones. Based on the BI and FI estimates, the top part of the Turonian is a more suitable candidate for hydrofracturing. A present-day stress state has been inferred from 1D mechanical earth modeling. The constrained SHmax magnitude range indicates a normal faulting stress state in weaker rocks with low UCS, whereas compressive failures in stronger rocks (70 MPa UCS) indicate a strike-slip state. Based on the geomechanical assessment, a safe wellbore trajectory analysis has been presented. Fracture reactivation potential during hydraulic stimulation is inferred, where in a normal faulting scenario, a minimum of 950 PSI additional pore pressure will be needed to reactivate optimally oriented natural fractures. The requirement is much less in a strike-slip regime. Considering μ = 0.6, fracture orientations of 10–30° N

and 130–150° N can be reactivated with a <500 PSI pressure increment. Clay materials within fractures are capable of reducing μ, and considering μ = 0.5, we observe the orientations of critically stressed fractures as 20–30° N and 130–140° N, while ~500 PSI pressure enhancement by fluid injection can cause slippage on a wide range of fracture orientations. To build a confident field-scale geomechanical model, calibration data is tremendously important. We recommend recording an extended leak-off test or mini-frac test to infer the fracture closure pressure within the Turonian carbonates, which will provide a confident estimate of the Shmin gradient. Coring and rock-mechanical testing provide static elastic properties and strength, so they are highly recommended in future wells encountering the Turonian section. That way, we can further validate the elastic property-based BI estimates. However, coring and lab testing are time-consuming processes and incur additional costs. The outcome of this study sheds critical insights on the unconventional reservoir properties and necessary strategies for unconventional reservoir development in the southeastern Constantine Basin.

Author Contributions: Conceptualization, R.B., S.S. and A.E.R.; methodology, R.B., S.S. and A.E.R.; software, R.B., S.S. and A.E.R.; validation, R.B., S.S. and A.E.R.; formal analysis, R.B., S.S. and A.E.R.; investigation, R.B., S.S. and A.E.R.; resources, R.B., S.S. and A.E.R.; data curation, R.B., S.S. and A.E.R.; writing—original draft preparation, R.B., S.S. and A.E.R.; writing—review and editing, R.B., S.S. and A.E.R.; visualization, R.B., S.S. and A.E.R.; supervision, R.B., S.S. and A.E.R.; project administration, R.B., S.S. and A.E.R.; funding acquisition, R.B., S.S. and A.E.R. All authors have read and agreed to the published version of the manuscript.

Funding: This research was funded the funding provided by the Priority Research Area Anthropocene under the program "Excellence Initiative—Research University" at the Jagiellonian University in Kraków. Dr. Ahmed E. Radwan is thankful to the Faculty of Geography and Geology, Institute of Geological Sciences, Jagiellonian University for the open-access funding of this publication.

Data Availability Statement: Not applicable.

Acknowledgments: The authors are grateful to Sonatrach Exploration Company, Algeria, for the data set and for permission to publish this work. This work is supported by the Direction of Higher Education and the Algerian Scientific Research Ministry (no. 613_DGRSDT). This research was funded by the Priority Research Area Anthropocene under the program "Excellence Initiative—Research University" at the Jagiellonian University in Kraków.

Conflicts of Interest: The authors declare no conflict of interest.

References

1. Herbin, J.P.; Montadert, L.; Muller, C.; Gomez, R.; Thurow, J.; Wiedmann, J. Organic-Rich Sedimentation at the Cenomanian-Turonian Boundary in Oceanic and Coastal Basins in the North Atlantic and Tethys. *Geol. Soc. Lond. Spec. Publ.* **1986**, *21*, 389–422. [CrossRef]
2. Klemme, H.D.; Ulmishek, G.F. Effective petroleum source rocks of the world: Stratigraphic distribution and controlling depositional factors. *AAPG Bull.* **1991**, *75*, 1809–1851. [CrossRef]
3. Lüning, S.; Kolonic, S.; Belhadj, E.M.; Belhadj, Z.; Cota, L.; Barić, G.; Wagner, T. Integrated depositional model for the Cenomanian–Turonian organic-rich strata in North Africa. *Earth-Sci. Rev.* **2004**, *64*, 51–117. [CrossRef]
4. Boutaleb, K.; Baouche, R.; Sadaoui, M.; Radwan, A.E. Sedimentological, petrophysical, and geochemical controls on deep marine unconventional tight limestone and dolostone reservoir: Insights from the Cenomanian/Turonian oceanic anoxic event 2 organic-rich sediments, Southeast Constantine Basin, Algeria. *Sediment. Geol.* **2022**, *429*, 106072. [CrossRef]
5. Farouk, S.; Sen, S.; Ganguli, S.S.; Ahmed, F.; Abioui, M.; Al-Kahtany, K.; Gupta, P. An integrated petrographical, petrophysical and organic geochemical characterization of the Lower Turonian Abu Roash-F carbonates, Abu Gharadig field, Egypt—Inferences on self-sourced unconventional reservoir potential. *Mar. Pet. Geol.* **2022**, *145*, 105885. [CrossRef]
6. Zobaa, M.K.; Oboh-Ikuenobe, F.E.; Ibrahim, M.I.; Arneson, K.K.; Browne, C.M.; Kholeif, S. The Cenomanian/Turonian oceanic anoxic event in the Razzak #7 oil well, north Western Desert, Egypt: Palynofacies and isotope analyses. In Proceedings of the 2009 GSA Annual Meeting 2009, Abstracts with Programs, Portland, OR, USA, 19 October 2009; p. 513.
7. Dokka, A.M.; Guellati, N.; Hamel, A. Cenomanian–Turonian carbonate reservoirs of Guerguett-El-Kihal, a new discovery in the Southeast Constantine Basin, Algeria. In Proceedings of the AAPG Annual Convention and Exposition, San Francisco, CA, USA, 3–6 June 1990.

8. Boudjema, A.; Rahmani, A.; Belhadj, E.M.; Hamel, M.; Bourmouche, R. Source rock identification and oil generation related to trap formation: Southeast Constantine Oil Field. In Proceedings of the Annual Convention, AAPG Annual Convention, San Francisco, CA, USA, 3–6 June 1990.
9. Baouche, R.; Sen, S.; Ganguli, S.S.; Boutaleb, K. Petrophysical and geomechanical characterization of the Late Cretaceous limestone reservoirs from the Southeastern Constantine Basin, Algeria. *Interpretation* **2021**, *9*, SH1. [CrossRef]
10. Askri, H.; Belmecheri, A.; Benrabah, B.; Boudjema, A.; Boumendjel, K.; Daoudi, M.; Drid, M.; Ghalem, T.; Docca, A.M.; Ghandriche, H.; et al. Geology of Algeria. In *Well Evaluation Conference Algeria*; Schlumberger: Houston, TX, USA, 1995; pp. 1–93.
11. Bentaalla-Kaced, S.; Aïfa, T.; Deramchi, K. Organic-rich Albian deposits as the origin of hydrocarbons-contaminated phosphates, southeast Constantine Basin, Algeria. *J. Pet. Sci. Eng.* **2017**, *157*, 680–695. [CrossRef]
12. Choquette, P.W.; Pray, L.C. Geologic nomenclature and classification of porosity in sedimentary carbonates. *AAPG Bull.* **1970**, *54* (Suppl. 2), 207–250.
13. Dunham, R.J. Classification of carbonate rocks according to depositional texture. *Am. Assoc. Pet. Geol. Mem.* **1962**, *1*, 108–121.
14. Embry, A.F.; Klovan, J.E. Absolute water depth limits of Late Devonian paleoecological zones. *Geol. Rundsch.* **1972**, *61* (Suppl. 2), 672–686. [CrossRef]
15. Flügel, E. *Carbonate Rocks. Analysis, Interpretation and Application*, 2nd ed.; Springer: Berlin/Heidelberg, Germany; New York, NY, USA, 2010. [CrossRef]
16. Jannot, Y.; Lasseux, D. A new quasi-steady method to measure gas permeability of weakly permeable porous media. *Rev. Sci. Instrum.* **2012**, *83* (Suppl. 1), 015113. [CrossRef] [PubMed]
17. Zoback, M.D. *Reservoir Geomechanics*; Stanford University: Stanford, CA, USA, 2007.
18. Abdelghany, W.K.; Radwan, A.E.; Elkhawaga, M.A.; Wood, D.A.; Sen, S.; Kassem, A.A. Geomechanical modeling using the depth-of-damage approach to achieve successful underbalanced drilling in the Gulf of Suez Rift Basin. *J. Pet. Sci. Eng.* **2021**, *202*, 108311. [CrossRef]
19. Radwan, A.; Sen, S. Stress path analysis for characterization of in situ stress state and effect of reservoir depletion on present-day stress magnitudes: Reservoir geomechanical modeling in the Gulf of Suez Rift Basin, Egypt. *Nat. Resour. Res.* **2021**, *30*, 463–478. [CrossRef]
20. Radwan, A.E.; Sen, S. Characterization of in-situ stresses and its implications for production and reservoir stability in the depleted El Morgan hydrocarbon field, Gulf of Suez Rift Basin, Egypt. *J. Struct. Geol.* **2021**, *148*, 104355. [CrossRef]
21. Militzer, H.; Stoll, R. Einige Beitrage der geophysik zur primadatenerfassung im Bergbau. *Neue Bergbautech.* **1973**, *3*, 21–25.
22. Grieser, W.V.; Bray, J.M. Identification of production potential in unconventional reservoirs. In Proceedings of the Production and Operations Symposium 2007, Oklahoma City, OK, USA, 31 March 2007. [CrossRef]
23. Jin, X.; Shah, S.N.; Roegiers, J.-C.; Zhang, B. An integrated petrophysics and geomechanics approach for fracability evaluation in shale reservoirs. *SPE J.* **2015**, *20*, 518–526. [CrossRef]
24. Enderlin, M.B.; Alsleben, H. A method for evaluating the effects of confining stresses and rock strength on fluid flow along the surfaces of mechanical discontinuities in low-permeability rocks. In *Shale Reservoirs—Giant Resources for the 21st Century: AAPG Memoir 97*; Breyer, J.A., Ed.; APPG: Tulsa, OK, USA, 2012.
25. Zoback, M.D.; Lund Snee, J.-E. Predicted and observed shear on preexisting faults during hydraulic fracture stimulation. *SEG Tech. Program Expand. Abstr.* **2018**, *239*, 3588–3592.
26. Almalikee, H.; Sen, S. Rock-mechanical properties and in situ stress state of the Upper Cenomanian Mishrif limestone reservoir, Zubair oil field, southern Iraq. *Interpretation* **2022**, *10*, T521–T529. [CrossRef]
27. Agbasi, O.E.; Sen, S.; Inyang, N.J.; Etuk, S.E. Assessment of pore pressure, wellbore failure and reservoir stability in the Gabo field, Niger Delta, Nigeria—Implications for drilling and reservoir management. *J. Afr. Earth Sci.* **2021**, *173*, 104038. [CrossRef]
28. Kassem, A.; Sen, S.; Radwan, A.E.; Abdelghany, W.K.; Abioui, M. Effect of depletion and fluid injection in the Mesozoic and Paleozoic sandstone reservoirs of the October oil field, Central Gulf of Suez Basin: Implications on drilling, production and reservoir stability. *Nat. Resour. Res.* **2021**, *30*, 2587–2606. [CrossRef]
29. Radwan, A.E. A multi-proxy approach to detect the pore pressure and the origin of overpressure: An example from the Gulf of Suez Rift Basin. *Front. Earth Sci.* **2022**, 1607. [CrossRef]
30. Bashmagh, N.M.; Lin, W.; Murata, S.; Yousefi, F.; Radwan, A.E. Magnitudes and Orientations of Present-Day In-Situ Stresses in the Kurdistan Region of Iraq: Insights into combined strike-slip and reverse faulting stress regimes. *J. Asian Earth Sci.* **2022**, *147*, 105398. [CrossRef]
31. Radwan, A.E.; Abdelghany, W.K.; Elkhawaga, M.A. Present-day in-situ stresses in Southern Gulf of Suez, Egypt: Insights for stress rotation in an extensional rift basin. *J. Struct. Geol.* **2021**, *147*, 104334. [CrossRef]